Effective Meshing and Form Factor Calculation for Accurate Progressive Radiosity

Wang-Yeh Lee * Jung-Hong Chuang
Department of Computer Science and Information Engineering
National Chiao Tung University
Hsinchu, Taiwan, Republic of China
{wylee, jhchuang}@csie.nctu.edu.tw

Abstract

In this paper, two effective methods are proposed to address two inaccuracies, deficient meshing and error-prone form factors, respectively, in the context of progressive radiosity. The first one addresses the meshing problem using an automatic adaptive subdivision that takes the radiosity difference, the radiosity residual, and the visibility information as error estimates. The second method employs a hybrid form-factor evaluation recursively combining an approximation to the analytic point-to-disk form factor and an accurate form factor from a differential area to a convex polygon. Finally, we demonstrate the effectiveness and practicability of the proposed methods by testing with a set of global illumination test scenes to show the experimental results qualitatively and quantitatively.

1. Introduction

The radiosity method simulates the transport of light between diffusely reflecting surfaces in an enclosure, thereby accounting for the global lighting effects. This method, borrowed from thermal engineering [17], first presented to the computer graphics community by Goral et al. [8] and Nishita et al. [14], respectively, has proven to be a viable approach for generating *view-independent* realistic computer images. Under some restricted assumptions, the well-known radiosity equation was formulated as:

$$B_i = E_i + \rho_i \sum_{j=1}^{n} B_i F_{ji},$$

where B_i is the radiosity of patch i, E_i is the emitted radiosity of patch i, ρ_i is the reflectivity of patch i, n is the number of patches in the scene, and F_{ij} is the form factor from patch i to patch j.

The resultant system of simultaneous radiosity equations can be solved using relaxation methods such as Gauss-Seidel and Southwell iterations. Unfortunately, most current solutions to the radiosity equation suffer from the inherent inaccuracies [3, 25, 2, 23] due to basic assumptions of the radiosity equation and the approximate method for evaluating form factors, usually resulting in jagged shadows, light/shadow leaking, Mach bands, and darker edges where surfaces meet. The intrinsic assumption of the radiosity equation states that the surfaces in the environment are broken down into a finite number of patches across which radiosity takes an uniform value. Therefore, the accuracy of the computation is determined by the discretization of the scene adapted to the light changes [24, 18, 21, 9, 12, 13]. On the other hand, form factor computation [22, 15, 16] is generally the approximate quadrature methods for evaluating the double integral of form factor F_{ij}, with which there is no general analytic solution available. Moreover, lying at the heart of the radiosity equation, the accurate computation of form factors determines the quality of the radiosity solution. To overcome the former inaccuracy, the finer mesh resulting from the large number of patches is needed to capture subtle lighting details while to overcome the latter, a highly accurate form-factor evaluation method must be tightly coupled within the framework of radiosity computation.

In this paper, two effective methods are proposed to address these two inaccuracies, deficient meshing and error-prone form factors, respectively, in the context of progressive radiosity (PR) [4]. The first one addresses the meshing problem using an automatic adaptive subdivision that takes the radiosity difference, the radiosity residual, and the visibility information as error estimates in a fashion that takes both effectiveness and cost into account. The second method employs a hybrid form-factor calculation combining an approximation to the analytic point-to-disk form fac-

* To whom all correspondence should be addressed.

Proceedings of the Theory and Practice of Computer Graphics 2004 (TPCG'04)
0-7695-2137-1/04 $20.00 © 2004 IEEE

tor and the 100% accurate form factor from a differential area to a convex finite area (patches). This hybrid method, tightly coupled and used in the PR framework, computes an approximation to the analytic point-to-disk form factor in a normal manner until the *five-times rule* assumption is violated. For these special cases, the accurate analytic form factor is alternately evaluated.

Finally, we demonstrate the effectiveness and practicability of the proposed methods by benchmarking with the entire set of global illumination test scenes [20] to show the experimental results qualitatively and quantitatively.

2. Progressive Radiosity Testbed

There are a number of commercial and freely distributed rendering softwares, which all exclusively employ progressive radiosity (PR) algorithms [4] for pre-calculation of shadows and lighting. The advantage of PR is well known that it is simple to implement, easy to control the simulation, and can produce an acceptable result in a desired time.

The radiosity solution to PR is solved incrementally by repeatedly selecting a shooting patch with the maximum energy and adding its contribution to the vertices of all elements in the environment. The radiosity in each element can be bilinearly interpolated directly from the element vertices. Thus the precomputed intensities from the radiosity computation can be used for interactive walkthroughs of the synthetic environment. The proposed two methods are both integrated in the context of progressive radiosity that uses ray-traced form-factor method [25] to numerically integrate the form factor.

2.1. Computing a Visibility Index

As for the form factor evaluation, at each vertex, the shooting patch is sampled adaptively, and for each sample point, a ray is cast to determine the visibility. As a result, the form factor from the element vertex to the shooting patch can be computed as an area-weighted average of point-to-disk form factors:

$$F_{dA_r \to A_s} = \frac{A_s}{n} \sum_{i=1}^{n} \delta_i \frac{\cos\theta_{si} \cos\theta_{ri}}{\pi {r_i}^2 + A_s/n}, \qquad (1)$$

where n is the number of sample point on A_s; r_i is the distance between dA_r and dA_{si}; θ_{si} is the the angle between normal at dA_{si} and direction to dA_r; θ_{ri} is the angle between normal at dA_r and direction to dA_{si}. Involved in the process of evaluation, an area-weighted average of visibility value can then be obtained. Thus at each shooting step, a shooting-patch *visibility index* [18, 19] can be stored with each vertex. The visibility information can be of great use to the proposed adaptive meshing method.

3. Automatic Adaptive Meshing

The radiosity across a patch is generally computed by hardware Gouraud interpolation using vertices of the mesh, which means that the accuracy of the radiosity solution depends on the size of the mesh elements. Meshing algorithms that use knowledge of the function to be approximated can be characterized as either *a priori* or *a posteriori*. The discontinuity meshing algorithm [12, 9, 21] computes the exact umbra and penumbra regions *a priori*, but is computationally costly thus not being practical in most applications. Typically, *a posteriori* meshing algorithms [6, 24, 11] for radiosity using h-refinement [7] is required to improve on accuracy of computation.

Our proposed meshing approach in the context of PR performs on demand the adaptive meshing at each successive shooting step in which decisions on which area to subdivided are based on the results of current shot. The main focus here is to effectively adapt to the scene luminance using more aggressive strategies with slightly extra cost. The local error estimation in our method based on nodal difference, nodal residual, and visibility information is much more likely to detect regions where bilinear interpolation cannot capture the variations in radiance, but yet keep low the number of subdivided elements. Our method proceeds using three subdivision criteria in turn for each element i to be subdivided:

1. Compute the n differences $(d_{ij})_{j=1,\ldots,n}$ of the nodal value at each vertex of element i with n vertices. If the maximum of $(d_{ij})_{j=1,\ldots,n}$ is greater than the user-specified threshold ϵ_d, then subdivide the element into four sub-elements and recursively preform the meshing process for each newly created element; else proceed with criterion 2.

2. Compute the residual r_i at the centroid of element i. If r_i is greater than the user-specified threshold ϵ_r, then subdivide the element into four sub-elements and recursively preform the meshing process for each newly created element; else proceed with criterion 3.

3. Evaluate the visibility indices at the center of element i and the midpoint of each of its n edges. Use these $n+1$ new visibility indices as well as the *n* visibility indices at vertices of the element already obtained during the shooting step to detect true shadow boundaries. If the maximum difference of these $2n+1$ visibility indices reaches the user-specified threshold ϵ_v, then subdivide the element and recursively preform the meshing process; else terminate the meshing process.

Evaluating these three criteria is in order of ascending computational complexity. This organization of evaluation order is aimed to be as relevant as to strike the balance of

cost and effectiveness for meshing. Although, the last criterion is the most costly and aggressive, it cannot be evaluated until all of the other two fails to pass the subdivision test. This way brings the proposed meshing algorithm a good assortment of computational efforts, effectiveness, and even accuracy in a user-controllable manner, thus reaching a more accurate radiosity computation.

4. Accurate Computation of Form Factors

The form factor plays a very crucial role in the radiosity simulation. The form factor between patches P_i and P_j can be described as a double integral formula:

$$F_{ij} = \frac{1}{A_i} \int_{x \in P_i} \int_{y \in P_j} \frac{\cos\theta \cos\theta'}{\pi r^2} \delta(x,y) dy dx,$$

where r is the distance between dx and dy; θ the angle between the normal to the surface at dx and the direction from dx to dy; θ' the angle between the normal to the surface at dy and the direction from dy to dx; and $\delta(x,y)$ is a visibility term taking the value 1 if dx is visible from dy and 0 otherwise. Such computations not only constitute the bulk of the computational efforts, but also have great impact on the accuracy of the radiosity simulation. Consequently, the quest of faster and/or accurate form-factor algorithms [5, 3, 25, 22, 15, 16] is an area of active research. Under the assumptions imposed by different frameworks of radiosity computation, form-factor evaluation algorithms should be carefully devised.

4.1. Hybrid Form-Factor Evaluation

In our proposed method, normal ray-traced form factor method using an approximation to the analytic solution of the point-to-disk form factor is applied in the context of PR. As shown in Equation (1), this *only* represents an approximation to the analytic point-to-disk form factor, since the angles can vary across the disk. As long as the distance between the point and the disk is large relative to the disk's size, this remains a second order approximation. Accordingly, violation of the proximity assumption that surfaces are far away from each other, relative to their sizes, however, should be effectively detected. To remedy this, an analytic formula for the form factor from a differential area to a convex polygon, instead, is used under the condition of close proximity. The 100% accurate form factor can be computed as a sum around the perimeter of the polygon using the following formula †:

$$F_{x,P} = -\frac{1}{2\pi} \sum_{g \in G} \vec{n} \cdot \vec{\Gamma}_g, \tag{2}$$

where $\vec{n}$ is the normal vector at the point x; G is the set of vertices of the polygon; $\vec{R}_g$ is a vector from x to vertex number g of patch P; and $\vec{\Gamma}_g$ is a vector with magnitude equal to the angle γ_g, between $\vec{R}_g$ and $\vec{R}_{g+1}$, and direction given by the cross product $\vec{R}_g \times \vec{R}_{g+1}$. The geometry for evaluating analytic form factors is shown in Figure 1.

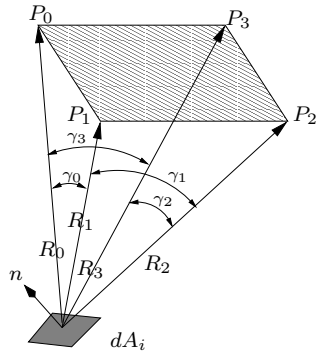

Figure 1. Geometry for evaluating analytic form factor from a differential area to a convex polygon.

Unfortunately, this formula does not take occlusion into account. This visibility function is a complicated non-linear factor in Equation (2) that can only be evaluated effectively using point sampling methods. However, in conjunction with the appropriate visibility algorithm, an exactly correct form factor can yet be obtained. A detailed derivation of Equation (2) can be found in [10].

By adaptively subdividing source patch into n smaller areas ΔA_i and using a different constant visibility (0 or 1) associated to the area, the visibility from the point of x to the source patch can be approximated to any degree of accuracy. Thus, the contribution of the source shooting patch s to a receiving point x at the element r can be formulated as

$$\begin{aligned} \Delta B_r(x) &= \rho_r B_s \sum_{i=1}^{n} \delta(i,x) F_{dA_r(x),\Delta A_i} \\ &= \rho_r B_s F^{\text{hybrid}}_{r(x),s}, \end{aligned} \tag{3}$$

where $\delta(i,x)$ is the visibility function from x to ΔA_i taking the value of either 0 or 1; $F_{dA_r(x),\Delta A_i}$ can be the form

† Note the minus sign in this formula. To the best of the authors's knowledge, relevant literature on the formula taking the positive sign would be erroneous.

factor formula of either Equation (1) or Equation (2); and $F^{\text{hybrid}}_{r(x),s}$ is a hybrid combination of numerical and analytic form factors considering visibility.

The selection of the formulae used for $F_{dA_r(x),\Delta A_i}$ in Equation (3) lies in determining whether the proximity assumption is violated, in which the closeness criterion using the *five-times rule* will be tested. This means that the exactly analytic formula of Equation (2) is only required and used in close proximity; otherwise, an approximation to the analytic point-to-disk form factor formula of Equation (1) is applied.

The *five-times rule* [1], which has been used by illumination engineers for nearly a century, states:

> A finite area Lambertian emitter should be modeled as a point source only when the distance to the receiving surface is greater than five times the maximum projected width of the emitter.

Put it in another way, if the *five-times rule* should be satisfied, an approximation using the point-to-disk form factor would be good enough in the radiosity simulation. But care must be taken not to lose the increased precision of the proposed form-factor evaluation method, since patch radiosities should be computed as a weighted average of vertex radiosities, which is some degree of approximation. Thus an appropriate meshing algorithm as our first proposed adaptive meshing method is a necessity to collaborate with an effective, accurate form-factor evaluation method for a higher accurate and effective radiosity computation.

4.2. Adaptive Source Sampling

In order to use Equation (3) to compute an accurate estimate of the contribution from the source shooting patch s to a receiving point x at the element r, patch s should be subdivided into a set of delta areas small enough to avoid visibility errors. Our proposed form-factor evaluation method employs adaptive sampling by concentrating the regions where the integrand varies the most.

The source adaptive sampling method use the following scheme: for each receiving vertex with respect to the shooting patch, if one of the following conditions holds; then split the sampling area of the shooting patch recursively until the split area $\Delta A_s \leq \epsilon_A$, where the tolerance ϵ_A is used to prevent excessive subdivision.

1. The difference between the form factor estimate obtained using the current sampling domain and that obtained using its 4 sampling sub-domains is greater than the user-specified threshold ϵ_{fd}.
2. The form factor estimate is greater than the user-specified threshold ϵ_{fe}.
3. The visibility index computed so far is neither full visible nor full invisible.

In conjunction with the adaptive source sampling, the proposed hybrid form-factor evaluation method *recursively* tests each pair of the resultant adaptively-subdivided subpatch and the receiving vertex against the *five-times rule* test. If the vertex-to-subpatch pair survives the test, then apply the approximate formula to the analytic point-to-disk form factor of Equation (1). Otherwise apply, instead, the analytic point-to-polygon form factor formula of Equation (2). Finally, the delta form factors including the visibility information of all the vertex-to-subpatch pairs are summed up by using Equation (3). Thus, a more effective and accurate radiosity contribution from the source shooting patch to each receiving vertices in the scene will be computed, whereas form factors evaluated by a *recursively* hybrid combination of two different form-factor formulae can be obtained.

5. Experimental Results

The progressive radiosity using the proposed meshing and form factor computation methods in this paper was implemented in C and OpenGL API on a Red Hat Enterprise Linux PC with a 3.2 GHz Pentium 4, 1 GByte main memory, and a nVidia Quadro FX 500 graphics board.

We exercised the proposed algorithms with all models from the entire set of five global illumination test scenes [20], in which each test scene has been designed to test different modes of light transport and as well stress different parts of a given renderer. These test scenes are all achromatic, as simple as possible, and still test a particular aspect of global transport algorithms.

The five test scenes we used are Emission, Shadow, Huge, Secondary, and Geometry test scenes, respectively. Statistics are presented in Table 1 to quantitatively illustrate the resultant information with regard to the number of shooting iteration, the numbers of input patches and resulting elements, the maximum depth of quadtree subdivision, the number of early automatic adaptive meshing performed, and the total rendering time. We show the runtime the proposed method took to generate the images for reference *only*, since algorithms should probably not be optimized for these tests, where in some aspects, efficiency issues may show up. Furthermore, we demonstrate the rendered images of the original test scene with wireframe, the image of radiosity solution using Gouraud interpolation, and the image showing the results of meshing for qualitative and visual comparison/validation.

In Figure 2, Emission test scene checks sampling algorithms and that the effect of 100 small lights on the right is equal to the single large light on the left. In Figure 3, Shadow test scene tests transfer in the presence of occluders and causes $D1$ shadow discontinuities by the orientation of the light on the ground. In Figure 4, Huge test scene

	Emission	Shadow	Huge	Secondary	Geometry
# of input patches	107	55	20	20	30
# of shooting iterations	120	3	5	5	2
Max quadtree depth of meshing	10	10	13	10	10
# of early iterations with meshing performed	120	1	3	2	1
# of resulting elements	44 171	32 983	34 790	58 325	16 386
Total rendering time (times in seconds)	140.37	126.53	12.18	237.53	20.11

Table 1. Statistics for five global illumination test scenes.

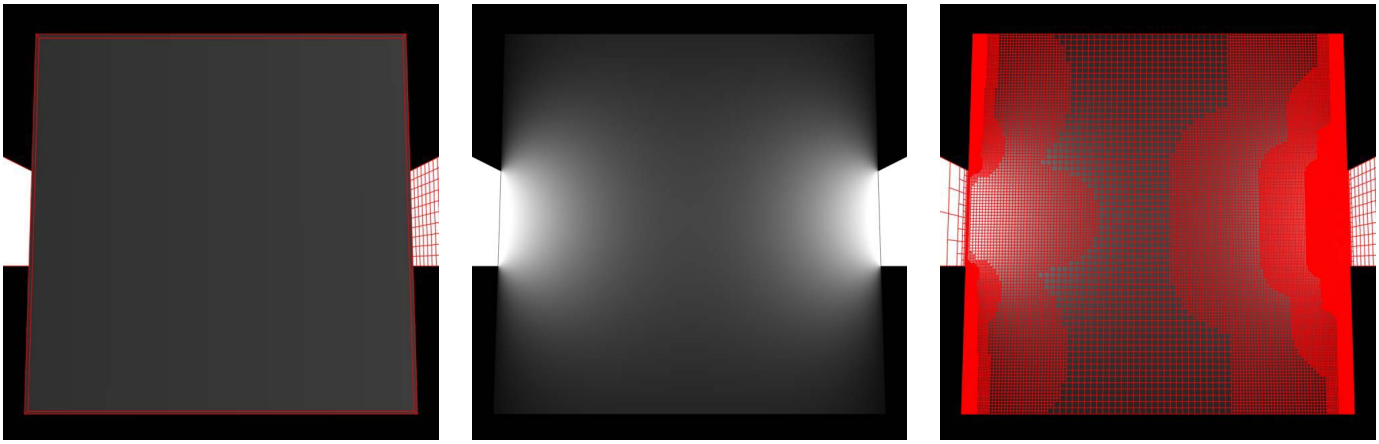

(a) Original test scene showing wireframe. (b) Image of radiosity solution. (c) Result of meshing.

Figure 2. Images of Emission test scene.

consists of a large ground plane, and two pairs of light and blocker with the same size. Underneath the larger pair is a smaller pair scaled down in width and depth by a factor of 10. This test scene stresses the capability of energy exchange in a large spatial extent from two emitters with luminance of enormous variation (99% of the energy is due to the large light, but much of visible energy is due to the small light). In Figure 5, Secondary test scene, which consists of a ground plane with a light underneath shining on a diffuse surface to the size of the ground plane, tests algorithms against complex illumination paths. All illumination on the visible regions is from the secondary luminaire. The final images shown in Figure 6 is Geometry test scene that puts emphasis on the geometry accuracy test, where three cubes and a wedge with a slightly rotation from alignment can check the robustness of meshing algorithms. These preliminary experimental results help to validate the effectiveness and accuracy of our proposed methods.

6. Concluding Remarks

This paper presented an automatic adaptive meshing and a hybrid form-factor evaluation method in the context of the most popular progressive radiosity algorithm to effectively address intrinsic inaccuracies in radiosity methods. The automatic adaptive meshing addresses the meshing problem using an automatic adaptive subdivision that takes the radiosity difference, the radiosity residual, and the visibility information as error estimates in a fashion that takes both effectiveness and cost into account. The hybrid form-factor evaluation method *recursively* combines an approximation to the analytic point-to-disk form factor and an accurate form factor from a differential area to a convex polygon in order to achieve a more accurate and effective form-factor evaluation.

We finally benchmarked the proposed methods against the entire set of global illumination test scenes and demonstrated rendered images with timing statistics to show the effectiveness and efficiency of the proposed methods, in hopes of allowing for bridging the gap between the theory

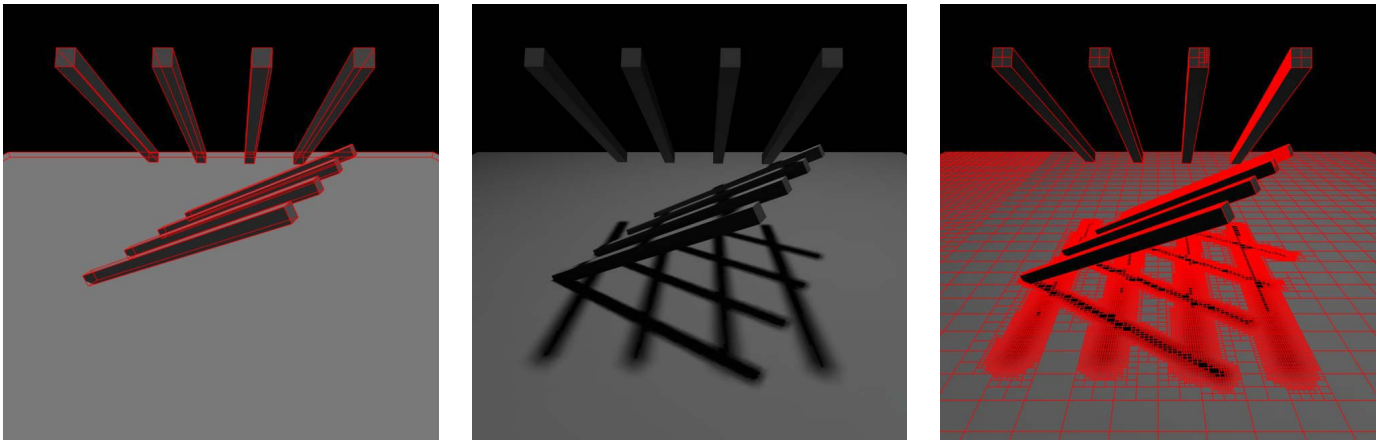

(a) Original test scene showing wireframe. (b) Image of radiosity solution. (c) Result of meshing.

Figure 3. Images of Shadow test scene.

(a) Original test scene showing wireframe. (b) Image of radiosity solution. (c) Result of meshing.

Figure 4. Images of Huge test scene.

and practicability, or applicability, of progressive radiosity methods.

7. Acknowledgments

We would like to thank the anonymous reviewers for their helpful comments and suggestions. This work was supported in part by grants from the National Science Council of the Republic of China under Contract No. NSC 91-2213-E-009-139.

References

[1] I. Ashdown. *Radiosity: A programmer's perspective*. John Wiley & Sons, 1994.

[2] D. R. Baum, S. Mann, K. P. Smith, and J. M. Winget. Making radiosity usable: automatic preprocessing and meshing techniques for the generation of accurate radiosity solutions. *Computer Graphics*, 25(4):51–60, 1991.

[3] D. R. Baum, H. E. Rushmeier, and J. M. Winget. Improving radiosity solutions through the use of analytically determined form-factors. *Computer Graphics*, 23(3):325–334, 1989.

[4] M. F. Cohen, S. E. Chen, J. R. Wallace, and D. P. Greenberg. A progressive refinement approach to fast radiosity image generation. *Computer Graphics*, 22(4):75–84, August 1988.

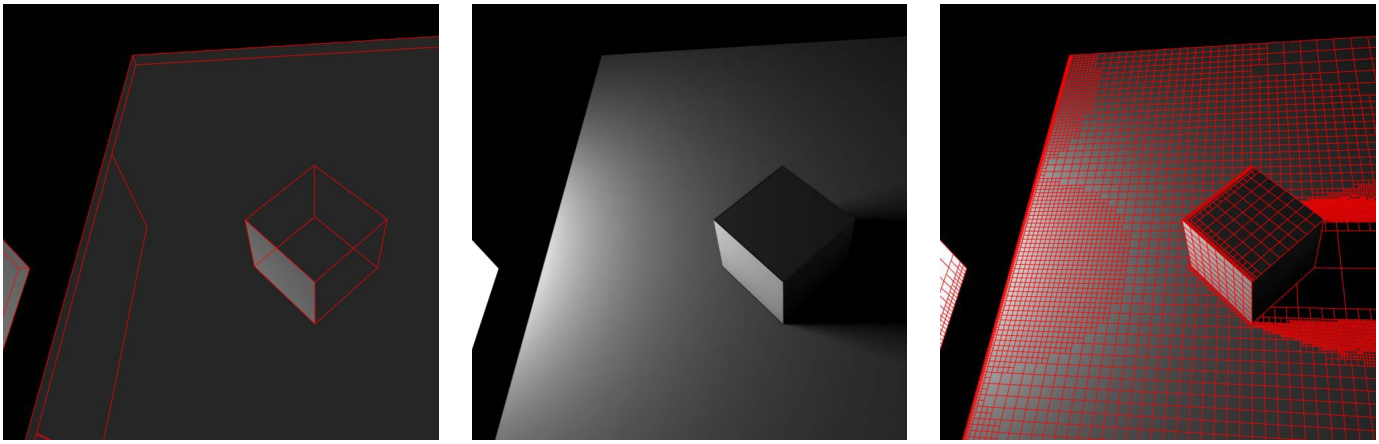

(a) Original test scene showing wireframe. (b) Image of radiosity solution. (c) Result of meshing.

Figure 5. Images of Secondary test scene.

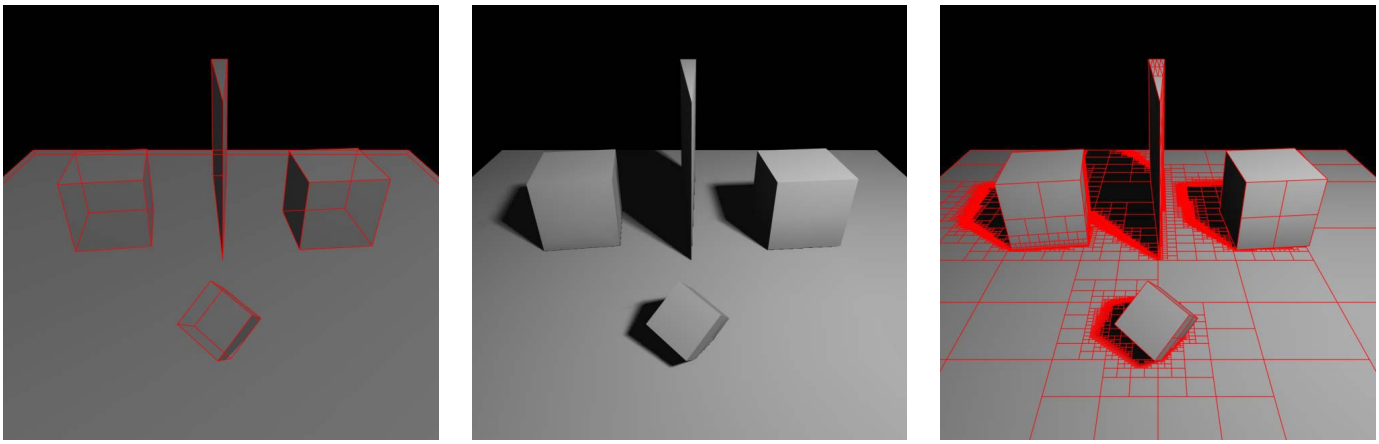

(a) Original test scene showing wireframe. (b) Image of radiosity solution. (c) Result of meshing.

Figure 6. Images of Geometry test scene.

[5] M. F. Cohen and D. P. Greenberg. The hemi-cube: A radiosity solution for complex environments. *Computer Graphics*, 19(3):31–40, July 1985.

[6] M. F. Cohen, D. P. Greenberg, and D. S. Immel. An efficient radiosity approach for realistic image synthesis. *IEEE Computer Graphics & Applications*, 6(2):26–35, 1986.

[7] M. F. Cohen and J. R. Wallace. *Radiosity and Realistic Image Synthesis*. Academic Press, 1993.

[8] C. M. Goral, K. E. Torrance, D. P. Greenberg, and B. Battaile. Modelling the interaction of light between diffuse surfaces. *Computer Graphics*, 18(3):212–222, 1984.

[9] P. S. Heckbert. Discontinuity meshing for radiosity. In *Third Eurographics Workshop on Rendering*, pages 203–216, Bristol, UK, May 1992.

[10] H. C. Hottel and A. F. Sarofin. *Radiative Transfer*. Mc Graw-Hill, New York, 1967.

[11] E. Languenou, K. Bouatouch, and P. Tellier. An adaptive discretization method for radiosity. *Computer Graphics Forum (EUROGRAPHICS '92)*, 11(3):C–205–C–216, 1992.

[12] D. Lischinski, F. Tampieri, and D. P. Greenberg. A discontinuity meshing algorithm for accurate radiosity. *IEEE Computer Graphics & Applications*, 12(4):25–39, 1992.

[13] D. Lischinski, F. Tampieri, and D. P. Greenberg. Combining hierarchical radiosity and discontinuity meshing. In J. T. Kajiya, editor, *SIGGRAPH 93 Conference Proceedings*, Computer Graphics Proceedings, Annual Conference Series, pages 199–208. ACM SIGGRAPH, ACM Press, August 1993.

0-7695-2137-1/04 $20.00 © 2004 **IEEE**

[14] T. Nishita and E. Nakamae. Continuous tone representation of three-dimensional objects taking account of shadows and interreflection. *Computer Graphics*, 19(3):23–30, 1985.

[15] G. Pietrek. Fast calculation of accurate formfactors. In *Proceedings of fourth Eurographics Workshop on Rendering*, pages 201–220, June 1993.

[16] P. Schröder and P. Hanrahan. On the form factor between two polygons. In *SIGGRAPH '93 Proceedings*, pages 163–164, August 1993.

[17] R. Siegel and J. R. Howell. *Thermal Radiation Heat Transfer*. Hemisphere Publishing, Washington, DC, 1981.

[18] F. X. Sillion. Detection of shadow boundaries for adaptive meshing in radiosity. In J. Arvo, editor, *Graphics Gems II*, pages 311–315. Academic Press, San Diego, 1991.

[19] F. X. Sillion and C. Puech. *Radiosity and Global Illumination*. Morgan Kaufmann, 1994.

[20] B. Smits and H. W. Jensen. Global illumination test scenes. Technical Report UUCS-00-013, University of Utah, 2000. http://www.cs.utah.edu/~bes/papers/scenes.

[21] W. Stürzlinger. Adaptive mesh refinement with discontinuities for the radiosity method. In *Proceedings of Fifth Eurographics Workshop on Rendering*, June 1994.

[22] F. Tampieri. Accurate form-factor computation. In D. Kirk, editor, *Graphics Gems III*, pages 329–333. Academic Press, San Diego, 1992.

[23] F. Tampieri and D. Lischinski. The constant radiosity assumption syndrome. In *Proceedings of Second Eurographics Workshop on Rendering*, May 1991.

[24] C. Vedel and C. Puech. Some experiments on adaptive subdivision for progressive radiosity. In *Proceedings of Second Eurographics Workshop on Rendering*, May 1991.

[25] J. R. Wallace, K. A. Elmquist, and E. A. Haines. A ray tracing algorithm for progressive radiosity. *Computer Graphics*, 23:315–324, 1989.